RSC Advances

RSC Publishing

PAPER

CO_2 separation applying ionic liquid mixtures: the effect of mixing different anions on gas permeation through supported ionic liquid membranes†

Cite this: *RSC Advances*, 2013, **3**, 12220

Liliana C. Tomé,[ab] David J. S. Patinha,[a] Carmen S. R. Freire,[b] Luís Paulo N. Rebelo[a] and Isabel M. Marrucho*[ab]

In order to increase flexibility in tailoring the permeability and selectivity of supported ionic liquid membranes (SILMs) for flue gas separation and natural gas purification, this work explores the use of ionic liquid mixtures. For that purpose, gas permeation properties of CO_2, CH_4 and N_2 in several binary ionic liquid mixtures based on a common cation ($[C_2mim]^+$) and different anions such as bis(trifluoromethyl sulfonyl)imide ($[NTf_2]^-$), acetate ($[Ac]^-$), lactate ($[Lac]^-$), dicyanamide ($[DCA]^-$) and thiocyanate ($[SCN]^-$) were measured at 293 K using a time lag apparatus. In addition to gas permeation results, the thermophysical properties of those mixtures, namely viscosity and density, were also determined so that trends between the two types of properties could be evaluated. The results show that mixing $[Ac]^-$ or $[Lac]^-$ with $[NTf_2]^-$ promotes the decrease of gas permeability and diffusivity of the SILMs based on those binary mixtures, essentially due to their high viscosities. The pure ionic liquids containing anions with nitrile groups, $[DCA]^-$ or $[SCN]^-$, and also their mixtures with $[C_2mim][NTf_2]$ exhibit permselectivities ranging from 19.1 to 23.0 for CO_2/CH_4, and from 36.6 to 67.8 for CO_2/N_2, as a consequence of a reduction in the CH_4 and N_2 permeabilities, respectively. Furthermore, it is shown that mixing anions with different chemical features allows variations in ionic liquid viscosity and molar volume that impact the gas permeation properties of SILMs, offering a clear pathway for the optimization of their CO_2 separation performances.

Received 17th March 2013,
Accepted 15th May 2013

DOI: 10.1039/c3ra41269e

www.rsc.org/advances

Introduction

The topic of global warming, largely associated with the rising concentration of anthropogenic CO_2, is arguably one of the most important environmental issues that our world faces today. CO_2 emissions have been increasing and currently the power sector is mainly responsible for CO_2 emissions, which are related to fuel combustion for generating energy or heat. The escalating level of atmospheric CO_2 and the urgent need to take action to prevent irreversible climate change have hugely increased efforts in the development of new efficient and economic technologies for carbon capture and storage.[1]

The most relevant current technologies used for the elimination of CO_2 from natural gas streams and power plants include absorption with amines, adsorption with porous solids, membrane and cryogenic separation,[2,3] where amine-based absorption is undoubtedly the most common and efficient technology. Even though it has advantages such as high reactivity and good absorption capacity, the use of amines involves several concerns related to their corrosive nature, volatility and high energy demand for regeneration.[4] Alternatively, membrane separation exhibits inherent advantages, including the small scale of the equipment, relative environmental safety, ease of incorporation into existing processes, low energy consumption and operating costs.[5]

Despite the large array of polymeric membranes for CO_2 separation developed during the last decades,[6] there are still drawbacks to be overcome, such as the low CO_2 permeability and selectivity of solid membranes. To circumvent this problem, supported liquid membranes have also been approached due to the high diffusion of gases in liquids when compared to solid membranes, leading to higher gas permeabilities.[7] Traditionally, in a supported liquid mem-

[a]*Instituto de Tecnologia Química e Biológica, Universidade Nova de Lisboa, Av. República, 2780 157 Oeiras, Portugal. E mail: imarrucho@itqb.unl.pt; Fax: +351 214411277; Tel: +351 214469444*

[b]*CICECO, Departamento de Química, Universidade de Aveiro, Campus Universitário de Santiago, 3810 193 Aveiro, Portugal*

† Electronic supplementary information (ESI) available: Experimental viscosities and densities, as well as the calculated molar volumes of the pure ionic liquids and their mixtures, in the temperature range between 293.15 and 343.15 K. Comparison of the density and viscosity data gathered in this work for pure ionic liquids with the literature at 298 K. Density values fitted as a function of temperature by the method of the least squares. Viscosity values fitted in function of temperature using Arrhenius equation. The calculated excess molar volumes and viscosity deviations of the ionic liquid mixtures are also presented. See DOI: 10.1039/c3ra41269e

brane, the selected solvent is immobilized into the pores of a solid membrane by capillary forces. Unfortunately, the long-term stability of the membrane can be affected by solvent depletion through evaporation at specific operating conditions such as high temperature and pressure differentials. In order to overcome this drawback, the most interesting strategy is the use of ionic liquids (ILs). Supported ionic liquid membranes (SILMs) have been studied owing to the intrinsic properties of ILs such as negligible volatility,[8] high thermal stability,[9] and low flammability,[10] making them ideal liquid phases for supported liquid membrane applications. SILMs not only guarantee minimal membrane liquid loss through solvent evaporation, but also allow more stable membranes due to the higher viscosity of ILs and greater capillary forces between the desired ionic liquid and the support membrane.[11,12]

There has been a growing interest in the use of ILs in supported liquid membranes, particularly for CO_2 separation, not only due to the high levels of solubility and selectivity of CO_2 in these fluids relative to the other gases, namely CH_4 and N_2,[13–16] but also because of the ability to tailor many of their physical and chemical properties by combining different cations and anions or by adding functional groups.[17,18] Consequently, several studies on the permeation properties of gases through SILM systems have explored the effect of the IL structure. Relating to the influence of the cation, a number of groups have investigated the gas permeation properties of different families of ILs (imidazolium,[19–30] phosphonium,[31,32] sulphonium,[32] pyridinium,[33] and ammonium[34]) and improved results were obtained for imidazolium-based SILMs in terms of permeability and selectivity. Other studies, also focused on imidazolium ILs, explored different structural variations of the cation in order to enhance CO_2 solubility and selectivity.[35–37] On the other hand, the performance of imidazolium-based ILs containing several different anions has also been evaluated. Anions such as bis(trifluoromethylsulfonyl)imide ($[NTf_2]$),[19,24,27,29] hexafluorophosphate ($[PF_6]$),[27,38] trifluoromethanesulfonate ($[CF_3SO_3]$),[19,24] dicyanamide ($[DCA]$),[19,24,39] tricyanomethane ($[C(CN)_3]$),[29,39] tetracyanoborate ($[B(CN)_4]$),[39,40] among others, have been tested and the results indicate that nitrile-containing anions promote an increase in both CO_2 permeability and CO_2/N_2 selectivity when compared to the $[NTf_2]$. In summary, it is important to emphasize that the ability to tailor the CO_2 affinity for the ionic liquid by combining different cations and anions is perhaps the most important feature of ILs for gas separation applications.

Recently, ionic liquid mixtures have been proposed as a mean to further increase flexibility and the fine-tune capacity of the physical and chemical properties of these remarkable compounds, providing an extra degree of freedom for the design of new solvents.[41,42] However, only a few works have explored gas solubilities in binary IL + IL mixtures. Finotello *et al.*[43] measured the CO_2, CH_4 and N_2 solubilities of $[C_2mim][NTf_2]$ and $[C_2mim][BF_4]$ mixtures and the results showed that this approach can be used to enhance CO_2 solubility selectivity due to the control over IL molar volume. Shiflett and Yokozeki demonstrated that an IL mixture containing equimolar amounts of $[C_2mim][TFA]$ and $[C_2mim][Ac]$ has a combination of both chemical and physical absorption effects.[44] Wang *et al.* showed that improvements in CO_2 absorption performance can be obtained by mixing a functional IL $[NH_2C_2mim][BF_4]$ with low viscosity ILs, namely $[C_2mim][BF_4]$ and $[C_4mim][BF_4]$.[45] Although the use of IL mixtures seems to be a promising strategy, CO_2 separation using SILMs has never been attempted before.

Furthermore, a quick search in the open literature on the subject of CO_2 solubility in ionic liquids shows a marked contrast either in terms of the number of publications or on the chemical diversity of the ILs researched. From amine inspired reactive ILs to aprotic heterocyclic anion ILs,[46] the most recent studies focus on task specific ILs by using basic anions, such as acetate,[47] amino acids,[48] imidazolide or pyrrolide.[49]

In this work, the CO_2, CH_4 and N_2 permeation properties of IL mixtures through supported ionic liquid membranes is researched. Taking into account that the anions of ILs have a stronger influence on CO_2 solubility than the cations[15,50] and that the CO_2 molecules have a larger affinity for anion *versus* cation associations,[16,51] this study examines IL + IL mixture systems with a common cation and different anions. Four ionic liquids based on the 1-ethyl-3-methylimidazolium cation combined with anions that have different CO_2 solubility behaviours (chemical solubility: acetate, lactate; physical solubility: dicyanamide and thiocyanate) were mixed with 1-ethyl-3-methylimidazolium bis(trifluoromethylsulfonyl)imide. In order to explore the CO_2 separation performance trends of IL mixtures, supported ionic liquid membranes with different proportions of each anion were prepared. Since generally permeability in SILMs scales with viscosity, while selectivity scales with molar volume, the thermophysical properties, namely density and viscosity, of the prepared IL + IL mixtures were also measured and discussed.

Results and discussion

The gas permeation properties of binary IL + IL mixtures with different molar fractions through supported liquid membranes were measured using a time-lag apparatus, which allows for the simultaneous determination of permeability and diffusivity. The structures of the pure ILs used and the composition description of the prepared binary mixtures are shown in Fig. 1 and Table 1, respectively. The viscosity and density of the pure ILs and the binary IL mixtures reported in Table 1 were measured in this work and a detail description of these data in a temperature range from 293.15 to 343.15 K is presented and discussed in supplementary information (ESI†).

The gas transport through a solid or a dense liquid membrane occurs according to a solution–diffusion mass transfer mechanism where the permeability (P) is related to solubility (S) and diffusivity (D) as follows:[52]

$$P = S \times D \quad (1)$$

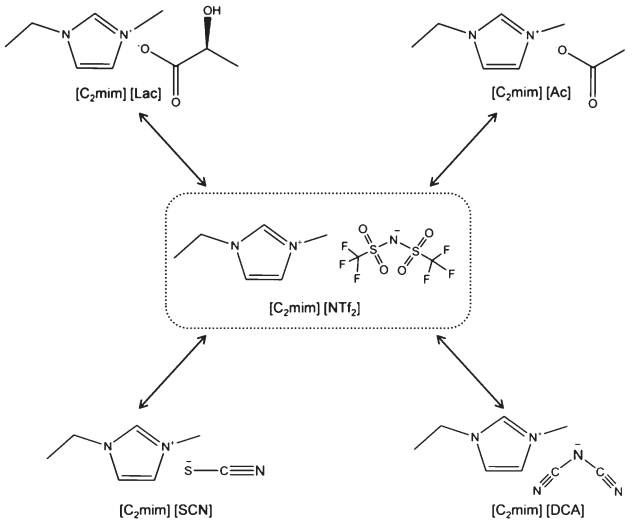

Fig. 1 Chemical structures and short names of the ionic liquids used in this work.

The gas permeability values were determined from the steady-state flux through the membrane (J), the membrane thickness (ℓ) and the pressure difference across the membrane (Δp) according to:

$$P = J\frac{\ell}{\Delta p} \quad (2)$$

The gas diffusivity (D) values were determined from the time-lag parameter (θ), which can be obtained before achieving steady state flux, using the following equation:[53]

$$D = \frac{\ell^2}{6\theta} \quad (3)$$

The ideal selectivity (or permselectivity), $\alpha_{A/B}$, was obtained by dividing the permeabilities of two different pure gases (A and B). The permselectivity is also a function of both the diffusivity selectivity and the solubility selectivity as follows:

$$\alpha_{A/B} = P_A/P_B = (S_A/S_B)\cdot(D_A/D_B) \quad (4)$$

Gas permeability and permselectivity

To the best of our knowledge, this is the first report on gas permeation properties of binary IL + IL mixtures supported membranes. Permeability and ideal permselectivity values of the prepared SILMs towards the measured gases are summarized in Table 2. A comparison of CO_2 permeability and CO_2/N_2 and CO_2/CH_4 permselectivities determined in this work with the values reported by Scovazzo *et al.* for $[C_2mim][DCA]$[19] and by Bara *et al.* for $[C_2mim][NTf_2]$[36] is shown in Table 3. These works were selected for comparison since the same experimental technique was used. The differences between CO_2 permeability and ideal permselectivities can be explained by the different measurement conditions, namely temperature and *trans*-membrane pressure differential as well as the different supports used (Table 3). Close *et al.*[30] have recently shown that the gas permeability through a SILM is influenced by the support membrane due to the difference between the IL interactions and the solid interfaces. Additionally, the presence of impurities or water in the IL greatly affect their physical[54,55] and gas permeation properties.[26] Since both Scovazzo *et al.*[19] and Bara *et al.*[36] did not report this information, an exact comparison cannot be made. These differences in results highlight the importance of measuring the properties of the pure ILs so that trends can be clearly established and comparisons between SILMs with pure ILs and their binary mixtures confidently performed.

Table 2 shows that the same trend of permeability values was observed for all the SILMs tested: P CO_2 > P CH_4 > P N_2 and, accordingly, α CO_2/N_2 is always greater than α CO_2/CH_4. In fact, the CO_2 permeability is always one or two orders of magnitude higher than that of CH_4 and N_2. Although the highest gas permeabilities were obtained for $[C_2mim][NTf_2]$-based SILM, the largest CO_2/CH_4 and CO_2/N_2 permselectivities of 23.0 and 67.8, respectively, were achieved for $[C_2mim][DCA]$. Actually, the CO_2 permeability of $[C_2mim][DCA]$ decreases 24%, while the CH_4 and N_2 permeabilities decrease 57 and 136%, respectively, compared to $[C_2mim][NTf_2]$ (Table 2). Thus, the highest permselectivities of $[C_2mim][DCA]$ are essentially due to the more pronounced decrease of CH_4 and N_2 permeabilities than that of CO_2. In addition, a similar

Table 1 Composition descriptions and physical properties of the pure ionic liquids and their mixtures used to prepare the SILMs studied

Ionic liquid sample	Composition (Mole fraction)	wt% of water	M (g mol^{-1})	η (mPa s)[a]	ρ (g cm^{-3})[a]	V_m (cm^3 mol^{-1})[b]
$[C_2mim][NTf_2]$	pure	0.02	391.31	39.085	1.524	256.78
$[C_2mim][NTf_2]_{0.75}[Ac]_{0.25}$	x $[C_2mim][NTf_2]$ 0.75 + x $[C_2mim][Ac]$ 0.25	0.08	336.04	60.936	1.451	231.55
$[C_2mim][NTf_2]_{0.5}[Ac]_{0.5}$	x $[C_2mim][NTf_2]$ 0.5 + x $[C_2mim][Ac]$ 0.5	0.14	280.76	98.011	1.362	206.17
$[C_2mim][NTf_2]_{0.25}[Ac]_{0.75}$	x $[C_2mim][NTf_2]$ 0.25 + x $[C_2mim][Ac]$ 0.75	0.48	225.49	127.927	1.249	180.53
$[C_2mim][Ac]$	Pure	0.49	170.21	164.930	1.101	154.61
$[C_2mim]$ $[NTf_2]_{0.5}[Lac]_{0.5}$	x $[C_2mim][NTf_2]$ 0.5 + x $[C_2mim][Lac]$ 0.5	0.37	295.77	103.633	1.365	216.64
$[C_2mim][Lac]$	Pure	0.54	200.23	370.413	1.145	174.87
$[C_2mim][NTf_2]_{0.5}[DCA]_{0.5}$	x $[C_2mim][NTf_2]$ 0.5 + x $[C_2mim][DCA]$ 0.5	0.12	284.26	29.169	1.362	208.66
$[C_2mim][DCA]$	Pure	0.09	177.21	17.947	1.106	160.24
$[C_2mim][NTf_2]_{0.5}[SCN]_{0.5}$	x $[C_2mim][NTf_2]$ 0.5 + x $[C_2mim][SCN]$ 0.5	0.04	280.28	38.600	1.371	204.39
$[C_2mim][SCN]$	Pure	0.09	169.25	27.846	1.119	151.24

[a] Viscosity (η) and density (ρ) measured at 293.15 K. [b] Molar volume (V_m) obtained for 293.15 K.

Table 2 Gas permeabilities (P) and ideal permselectivities (α) obtained in the prepared SILMs[a]

SILM sample	Gas permeability (Barrer)[b]				
	P CO_2	P CH_4	P N_2	α CO_2/CH_4	α CO_2/N_2
$[C_2mim][NTf_2]$	589 ± 1.0	32.5 ± 0.42	16.6 ± 0.11	18.1 ± 0.3	35.5 ± 0.3
$[C_2mim][NTf_2]_{0.75}[Ac]_{0.25}$	503 ± 1.8	28.3 ± 0.41	15.7 ± 0.28	17.8 ± 0.2	33.4 ± 0.7
$[C_2mim][NTf_2]_{0.5}[Ac]_{0.5}$	336 ± 3.4	18.9 ± 0.04	10.0 ± 0.10	17.7 ± 0.2	33.4 ± 0.7
$[C_2mim][NTf_2]_{0.25}[Ac]_{0.75}$	214 ± 0.4	12.6 ± 0.06	6.20 ± 0.19	17.0 ± 0.1	34.4 ± 1.1
$[C_2mim][Ac]$	118 ± 5.8	7.26 ± 0.24	3.25 ± 0.01	16.3 ± 1.3	36.4 ± 1.9
$[C_2mim]$ $[NTf_2]_{0.5}[Lac]_{0.5}$	265 ± 0.4	14.6 ± 0.19	7.20 ± 0.05	18.2 ± 0.3	36.8 ± 0.3
$[C_2mim][Lac]$	55 ± 0.3	3.13 ± 0.11	1.27 ± 0.01	17.6 ± 0.7	43.4 ± 0.6
$[C_2mim][NTf_2]_{0.5}[DCA]_{0.5}$	589 ± 1.9	30.9 ± 0.29	14.1 ± 0.18	19.1 ± 0.2	41.8 ± 0.7
$[C_2mim][DCA]$	476 ± 0.8	20.7 ± 0.01	7.03 ± 0.05	23.0 ± 0.1	67.8 ± 0.6
$[C_2mim][NTf_2]_{0.5}[SCN]_{0.5}$	516 ± 0.2	25.7 ± 0.07	14.1 ± 0.07	20.1 ± 0.1	36.6 ± 0.2
$[C_2mim][SCN]$	263 ± 0.6	12.1 ± 0.06	4.65 ± 0.15	21.8 ± 0.2	56.6 ± 1.9

[a] The listed uncertainties represent the standard deviations, based on three experiments. [b] Barrer (1 Barrer 10 ^{10} cm^3 (STP) cm cm^{-2} s^{-1} $cmHg^{-1}$).

result was also observed for the SILM made of pure $[C_2mim][SCN]$ due to identical decreases in the gas permeability values. This result demonstrates that the SILMs based on $[SCN]$ anions, whose experimental gas permeation properties are here reported for the first time, are capable of achieving high CO_2/N_2 permselectivities (Table 2). These findings are in line with other recently published studies, where ILs with other nitrile-containing anions lead to higher ideal CO_2/N_2 permselectivities compared to the $[NTf_2]$.[29,39,40]

Regarding the IL mixtures, mixing $[C_2mim][Ac]$ or $[C_2mim][Lac]$ with $[C_2mim][NTf_2]$ has a significant influence on the gas permeability properties of the SILMs. For instance, 0.5 molar fraction of $[C_2mim][Ac]$ in $[C_2mim][NTf_2]$ decreases CO_2, CH_4 and N_2 permeabilities by 75%, 72% and 66%, respectively while, for the 0.5 molar fraction of $[C_2mim][Lac]$, permeability decays of 122%, 123% and 130% occurred. In contrast, 0.5 molar fraction of $[C_2mim][SCN]$ just decreases 14%, 26% and 18% the CO_2, CH_4 and N_2 permeabilities, respectively. Moreover, 0.5 molar fraction of $[C_2mim][DCA]$ did not affect the CO_2 permeability and hardly affects the CH_4 and N_2 permeabilities compared to those of the pure $[C_2mim][NTf_2]$-based SILM.

The comparison of CO_2/CH_4 and CO_2/N_2 separation efficiencies between the results obtained in this work and the available data for SILMs is plotted in Fig. 2 in the form of Robeson plots.[6]

These plots, which are commonly used to evaluate the performance of membrane materials given a particular gas separation, demonstrate the compromise that exists between both the high selectivity and permeability. Robeson described the correlation as $P_i = k\alpha_{ij}^n$, where P_i is the permeability of the fastest gas, α_{ij}^n is the permselectivity, and n is the slope of the upper bound of the noted relationship.[6] Since the upper bound is based on large amounts of experimental data for each separation,[6] data points above this line can be considered as an improvement over the current membrane state of the art. Fig. 2(a) shows that the results obtained in this work for CO_2/CH_4 separation are bellow the upper bound, close to those available in literature for other pure ILs. However, SILMs made of pure $[C_2mim][Ac]$ and $[C_2mim][Lac]$ are exceptions since their CO_2/CH_4 separation performances fall in a empty data region of this plot, with much lower permeabilities than those obtained for other supported ionic liquid membranes. Regarding CO_2/N_2 separation, the SILM prepared with $[C_2mim][DCA]$ is above the upper bound, while the SILMs of the binary mixture $[C_2mim][NTf_2]_{0.5}[DCA]_{0.5}$ and the pure $[C_2mim][SCN]$ are on top of the line (Fig. 2(b)). Furthermore, Fig. 2(a) and Fig. 2(b) clearly show that the CO_2 separation performance of SILMs as a function of the permeability can be fine-tune by mixing different anions. For instance, mixtures of $[Ac]$ or $[Lac]$ with the $[NTf_2]$ anion causes a dramatic shift of the results along the x-axis without significantly sacrificing of the CO_2/CH_4 and CO_2/N_2 permselectivities. Thus, our results demonstrate that it is possible to adjust and design the SILMs permeability just by mixing anions which have different chemical natures and physical properties.

Table 3 Comparison of CO_2 permeability and ideal CO_2/N_2 and CO_2/CH_4 permselectivity values measured in this work to values reported in literature

	This work	Other works
$[C_2mim][NTf_2]$		Bara *et al.*[36]
Membrane support	PVDF	PES
Measurement conditions	293 K, 100 KPa	296 K, 85 kPa
P CO_2 (Barrer)	589	680
α CO_2/N_2	35.5	31
α CO_2/CH_4	18.1	14
η (mPa s)	39.085	N/A
Water content (wt%)	0.02	N/A
Purity (wt%)	99	N/A
$[C_2mim][DCA]$		Scovazzo *et al.*[19]
Membrane support	PTFE	PES
Measurement conditions	293 K, 100 KPa	303 K, 20 kPa
P CO_2 (Barrer)	476	610
α CO_2/N_2	68	61
α CO_2/CH_4	23	20
η (mPa s)	17.947	21
Water content (wt%)	0.09	N/A
Purity (wt%)	98	N/A

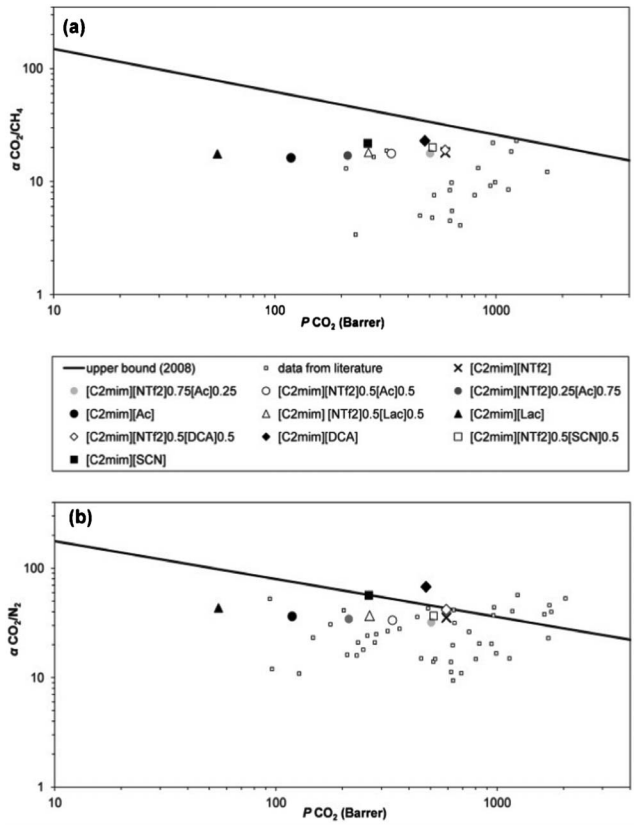

Fig. 2 Robeson plots of the studied gases in the prepared SILMs. Data are plotted on a log log scale and the upper bound for each gas pair is adapted from Robeson.[6] (a) CO_2/CH_4 permselectivity *versus* CO_2 permeability and (b) CO_2/CH_4 permselectivity *versus* CO_2 permeability. Literature data reported for other supported ionic liquid membranes are also plotted in (a)[24,31,34,36] and (b).[24,29,31,32,34,36,40,57,58]

Gas diffusivity

Gas diffusivity is a mass transfer property that affects gas permeability through SILMs as described by eqn (1). The higher the diffusivity, the faster the gas passes through the SILM. In general, ionic liquids that have larger viscosity will form SILMs with smaller permeability.[56] The experimental gas diffusivities obtained in this work at 293 K are plotted in Fig. 3.

The measured CO_2 diffusivity in $[C_2mim][NTf_2]$-based SILM is on the order of 10^{-10} m^2 s^{-1}, which is consistent with the values reported by other research groups.[21,59] From Fig. 3 it can be seen that the SILMs with lower gas diffusivities are $[C_2mim][Ac]$ and $[C_2mim][Lac]$, which also have the lowest gas permeabilities (Table 2) and the highest viscosities (Table 1). On the other hand, $[C_2mim][DCA]$ has the lowest viscosity but the highest gas permeabilities belong to $[C_2mim][NTf_2]$-based SILM. This means that not only the diffusivity plays an important role on gas permeability of SILM but the solubility should also be considered.

Scovazzo[21,31,34] and Baltus[33,59] have already showed that gas diffusivities in ILs are one or more orders of magnitude slower than in traditional solvents, essentially due to higher viscosities of ILs. Additionally, they also found that literature correlations for gas diffusivity in conventional solvents are inadequate to describe the gas diffusivity in ILs.[21,59] In view of that, several different correlations for gas diffusivity in different IL families have been developed considering the effect of temperature, solute molar volume, solvent viscosity, solvent density and solvent molecular weight.[21,31,33,34,59]

In Fig. 4(a) the relationship between gas diffusivity and IL viscosity, for the $[C_2mim][NTf_2][Ac]$ binary mixtures is shown. A wide range of viscosities was obtained for these mixtures, from 30 up to 170 mPa s. For the three studied gases, an increase in the mixture viscosity, due to the increment of $[C_2mim][Ac]$ molar fraction, corresponds to a decrease in the diffusivity. This behaviour, also observed for the mixture of $[C_2mim][NTf_2]_{0.5}[Lac]_{0.5}$ (Fig. 3 and Table 1), is similar to the previously proposed general trends observed for other pure

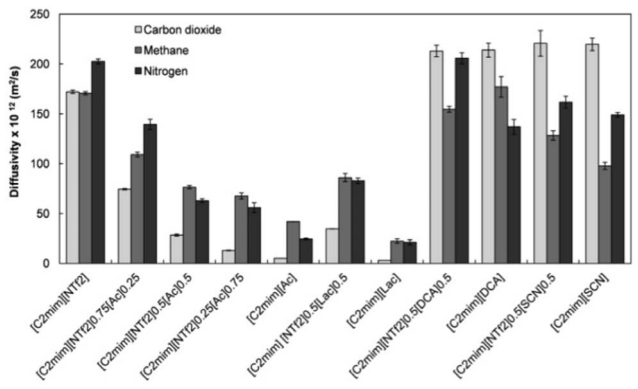

Fig. 3 Gas diffusivity through the prepared SILMs. Error bars represent standard deviations based on three experimental replicas.

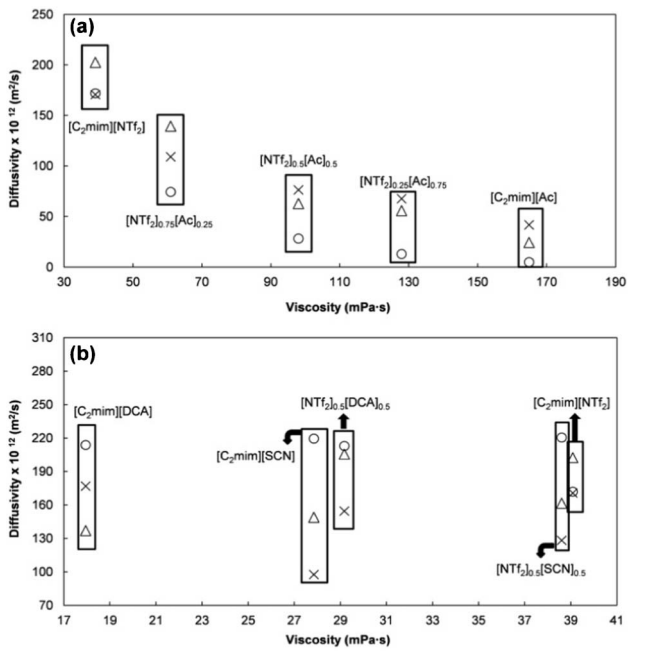

Fig. 4 Carbon dioxide (○), methane (×) and nitrogen (△) diffusivities in SILMs as function of measured IL viscosity.

SILMs.[21,31,34] In contrast, for the $[C_2mim][NTf_2]_{0.5}[SCN]_{0.5}$ and $[C_2mim][NTf_2]_{0.5}[DCA]_{0.5}$ mixtures different behaviours were found as shown in Fig. 4(b). Although the differences in viscosities, the presence of 0.5 molar fraction of $[C_2mim][NTf_2]$ in those two mixtures did not significantly affect their CO_2 diffusivity, whereas different changes in CH_4 and N_2 diffusivities compared to the pure $[C_2mim][DCA]$ and $[C_2mim][SCN]$ were observed. Furthermore, the results obtained in this work for pure $[C_2mim][NTf_2]$, $[C_2mim][DCA]$ and $[C_2mim][SCN]$ SILMs surprisingly showed that CH_4 and N_2 diffusivity trends follow unexpected sequences, from the highest to the lowest value, $[DCA] \sim [NTf_2] > [SCN]$ and $[NTf_2] > [DCA] \sim [SCN]$, respectively, contrasting to their viscosity trend $[NTf_2] > [SCN] > [DCA]$. This is a clear evidence that the description of the gas diffusivity in terms of IL viscosity only does not provide a full understanding of the different behaviours obtained since it is possible to have, for the same gas, different diffusivities in SILMs (pure IL or mixtures) that have the same viscosity.

Gas solubility

The CO_2, CH_4 and N_2 solubilities obtained in this work using eqn (1) are shown in Fig. 5. The same trend obtained for the permeability ($P\ CO_2 > P\ CH_4 > P\ N_2$) (Table 2), was also observed for the solubility for all the prepared SILMs: $S\ CO_2 > S\ CH_4 > S\ N_2$. From Fig. 5, it can be observed that $[C_2mim][Ac]$ exhibits the highest CO_2 solubility followed by $[C_2mim][Lac]$, surpassing the $[C_2mim][NTf_2]$-based SILMs. The addition of 0.5 molar fraction of $[C_2mim][Ac]$ or $[C_2mim][Lac]$ to $[C_2mim][NTf_2]$ increases 242% and 119% the CO_2 solubility, respectively, compared to the pure $[C_2mim][NTf_2]$. Conversely, 0.5 molar fraction of $[C_2mim][SCN]$ or $[C_2mim][DCA]$ promotes a CO_2 solubility decrease of 189% and 24%, respectively. It has been recognized that gas solubility in SILMs is related to IL molar volume.[60]

Two correlations for gas solubilities in ionic liquids based on the regular solution theory, with direct application to SILMs, have been proposed: Camper *et al.*[60] developed a model that uses only the molar volume of the IL to predict gas solubility and solubility selectivity, while Kilaru and Scovazzo proposed a two parameter model (the so-called Universal Model) that includes the IL molar volume and viscosity and covers an extended set of ionic liquid families.[61] The Camper Model was developed using only imidazolium-based ILs data with non-coordinating anions such as $[DCA]^-$, $[NTf_2]^-$, $[BF_4]^-$ or $[CF_3SO_3]^-$. According to this model, the solubility is given by:

$$S = \left\{ \left[\exp\left(\alpha + \frac{\beta}{(V_m)^{4/3}} \right) \right] V_m \right\}^{-1} \quad (5)$$

where α and β are gas specific parameters, S is the gas solubility (in moles of gas per liter of ionic liquid) and V_m is the IL molar volume. The solubility selectivity can be calculated by the ratio of eqn (5) solved for each gas in the gas pair. The result is a prediction of an exponential increase in solubility selectivity as the IL molar volume decreases.[60]

Fig. 6 displays the solubility selectivity values of the SILMs studied in this work *versus* IL molar volume, as well as the Camper Model. As can be clearly seen in Fig. 6(a) and Fig. 6(b), the CO_2/CH_4 and CO_2/N_2 solubility selectivity trends of the pure $[C_2mim][NTf_2]$, $[C_2mim][DCA]$, $[C_2mim][SCN]$ and their respective binary mixtures are in reasonable agreement with the Camper Model. For example, mixtures of different ILs, such as $[C_2mim][NTf_2]_{0.5}[DCA]_{0.5}$ and $[C_2mim][NTf_2]_{0.5}$

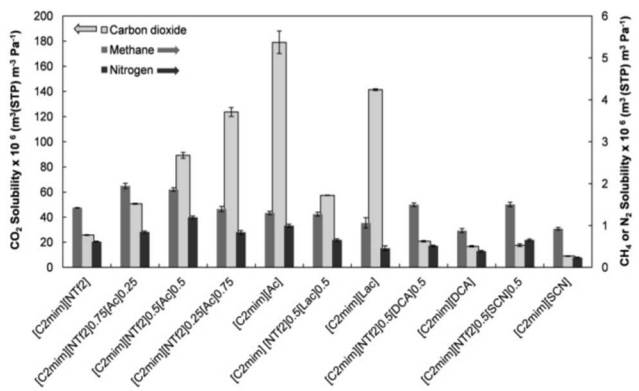

Fig. 5 Gas solubility in the SILMs studied, calculated using eqn (1). Error bars are standard deviations.

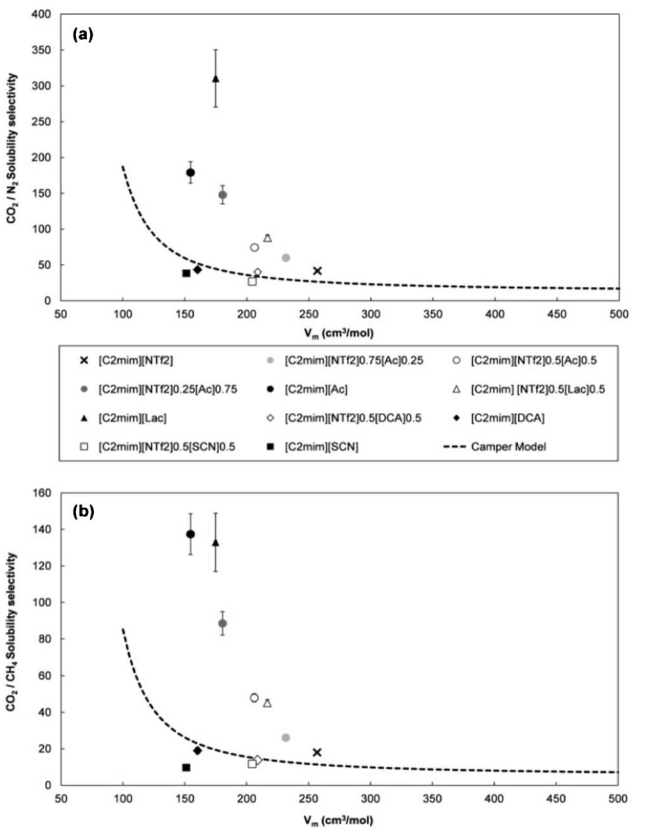

Fig. 6 Solubility selectivity of the prepared SILMs plotted *versus* IL molar volume. For both figures (a) and (b), the error is either within the size of the markers or shown by error bars. The dashed lines represent the solubility selectivity predicted by the Camper Model for each gas pair.[60]

$[SCN]_{0.5}$, with similar molar volumes, have roughly the same solubility selectivity which can be described by the Camper Model. Nevertheless, for $[C_2mim][Ac]$, $[C_2mim][Lac]$ and also for their binary mixtures with $[C_2mim][NTf_2]$, the Camper Model is not suitable to describe their CO_2/N_2 and CO_2/CH_4 solubility selectivities as shown in Fig. 6. It is well documented that the CO_2 solvation in $[C_2mim][Ac]$ occurs through a chemical reaction scheme, still not fully understood, which is responsible for the high solubility.[62–64] This contrasts with the physical solubility scheme observed for the ILs used in the derivation of the Camper Model. This means that the Camper Model is not a general model for imidazolium-based ILs, as claimed by the authors but, in fact, limited by the anion nature of the ILs used in its derivation or, in other words, limited to ILs where CO_2 physical solubility occurs. Deviations to the Camper Model,[60] and also to the Universal Model,[61] were observed for the CO_2/CH_4 solubility selectivity in imidazolium ILs combining alkylsulfate and alkylsulfonate anions.[65] The authors correlated these deviations with the low solubility of CH_4 in these ILs, which was explained using Kamlet–Taft β-parameter (the hydrogen bond donor capacity) that is governed by the anion basicity.

Interestingly, the solubility selectivity of CO_2 to CH_4 and N_2 in $[C_2mim][NTf_2]$-based SILMs can be enhanced by adding $[C_2mim][Ac]$ or $[C_2mim][Lac]$, as shown in Fig. 6. The addition of 0.25, 0.5 and 0.75 molar fraction of $[C_2mim][Ac]$ promote enhancements of 44%, 166% and 392% in the CO_2/CH_4 solubility selectivity, while for CO_2/N_2 increases of 44%, 78% and 254% were obtained. Moreover, 0.5 molar fraction of $[C_2mim][Lac]$ increases 150% the CO_2/CH_4 and 110% the CO_2/CH_4 solubility selectivity. Despite these CO_2 solubility selectivity enhancements in $[C_2mim][NTf_2]$ by mixing $[Ac]^-$ and $[Lac]^-$, the CO_2/N_2 and CO_2/CH_4 permselectivities did not drastically change (Table 2). This fact is essentially due to the decrease in diffusivity selectivity obtained for these IL mixtures, since for CO_2/N_2 diffusivity selectivity, values of 0.2 and 0.1 were obtained in the pure $[C_2mim][Ac]$ and $[C_2mim][Lac]$-based SILMs, respectively. Similarly, a CO_2/CH_4 diffusivity selectivity value of 0.1 was achieved for both SILMs. Given that, SILMs based on pure $[C_2mim][Ac]$ or $[C_2mim][Lac]$ and also their mixtures do not follow the usual behaviour that permselectivity in SILMs is essentially dominated by solubility selectivity. Actually, diffusivity selectivity in a SILM is expected to be proportional to the ratio of gas molar volumes (approximately one) as generally observed for SILMs performed with pure ILs.[56]

Conclusions

Permeability, diffusivity and solubility of CO_2, N_2 and CH_4 in different ionic liquid mixtures using supported liquid membrane configurations were measured at 293 K and 100 kPa using a time-lag apparatus. Results showed that ionic liquid mixtures is an easy and promising strategy to perform CO_2 separation using supported ionic liquid membranes, since the IL properties can be tuned by mixing anions with completely different chemical character.

The CO_2/CH_4 separation performance of all the SILMs prepared in this work is similar to that of SILMs containing only pure ionic liquids. Regarding CO_2/N_2 separation performance, the pure $[C_2mim][DCA]$ clearly exceeds the Robeson upper bound and both the $[C_2mim][NTf_2]_{0.5}[DCA]_{0.5}$ mixture and the pure $[C_2mim][SCN]$-based SILMs are on the upper bound, which makes them promising candidates for CO_2/N_2 separation applications.

The Camper Model provides a good description of the CO_2/CH_4 and CO_2/N_2 solubility selectivity values for the $[C_2mim][NTf_2][DCA]$ or $[C_2mim][NTf_2][SCN]$ mixtures. However, this model fails in describing the solubility selectivity of the $[C_2mim][NTf_2][Ac]$ or $[C_2mim][NTf_2][Lac]$ binary mixtures.

Even though higher CO_2 solubility selectivity improvements were obtained by mixing $[NTf_2]^-$ with $[Ac]^-$ or $[Lac]^-$, the CO_2/N_2 and CO_2/CH_4 permselectivities of those binary mixtures did not significantly change due to a significant decreased in the diffusivity selectivities. Nonlinear trends were found relating gas permeability and diffusivity with the viscosity, but the overall results showed that mixing ILs that have higher viscosities with $[NTf_2]^-$ decreases the gas permeability and diffusivity of the mixtures. In addition, the highest CO_2 separation performances were found for the less viscous mixtures of ionic liquids, meaning that a proper balance combining both the most selective and the less viscous anions is crucial to achieve improved CO_2 separation performances.

Experimental section

Materials

IoLiTec GmbH provided the 1-ethyl-3-methylimidazolium bis (trifluoromethylsulfonyl)imide ($[C_2mim][NTf_2]$), 99 wt% pure, 1-ethyl-3-methylimidazolium dicyanamide ($[C_2mim][DCA]$), >98 wt% pure, and 1-ethyl-3-methylimidazolium acetate ($[C_2mim][Ac]$), >95 wt% pure. Aldrich supplied the 1-ethyl-3-methylimidazolium L-(+)-lactate ($[C_2mim][Lac]$), $\geqslant$95 wt% pure. The 1-ethyl-3-methylimidazolium thiocyanate ($[C_2mim][SCN]$), $\geqslant$95 wt% pure, was purchased from Fluka. The chemical structures of the ILs used in this study are presented in Fig. 1.

To reduce the water and other volatile substances contents, all the pure IL samples were dried under vacuum (10^{-3} kPa) and subjected to vigorous stirring at a moderated temperature ($\approx$318 K) for at least 4 days immediately prior to use. The water contents of the pure ILs, determined by Karl Fischer titration (831 KF Coulometer, Metrohm), are presented in Table 1. The larger water contents for both the $[C_2mim][Ac]$ and $[C_2mim][Lac]$ are most probably due to the hydrophilic nature of their anions. No further purification of the ILs was carried out, but their purities were confirmed by ^1H RMN analysis.

Carbon dioxide (CO_2), nitrogen (N_2) and methane (CH_4) were supplied by Air Liquid and were of at least 99.99% purity. Gases were used with no further purification.

Preparation of the ionic liquid mixtures

The binary mixtures of IL + IL with different molar fractions were prepared using an analytical high-precision balance with an uncertainty of $\pm 10^{-5}$ g by syringing known masses of the IL components into glass vials. Good mixing was assured by magnetic stirring for at least 30 min. Then, the prepared IL mixtures were dried under vacuum (10^{-3} kPa) at a moderate temperature (≈ 318 K) for another 4 days. The samples were prepared immediately prior to the measurements to avoid variations in composition. The composition descriptions of the prepared IL + IL mixtures as well as their water contents determined by Karl Fischer titration are presented in Table 1.

Viscosity and density determination

Measurements of viscosity and density for the pure ILs and their mixtures were performed in the temperature range between 293.15 and 343.15 K at atmospheric pressure using an SVM 3000 Anton Paar rotational Stabinger viscometer-densimeter. This equipment uses Peltier elements for fast and efficient thermostability. The temperature uncertainty is ± 0.02 K. The precision of the dynamic viscosity measurements is $\pm 0.5\%$ and the absolute uncertainty of the density is ± 0.0005 g cm^{-3}. The overall uncertainty of the viscosity measurements (taking into account the purity and handling of the samples) was estimated to be 2%.[66] Further details on the equipment can be found elsewhere.[67] At least 3 measurements of each sample were performed to ensure accuracy and the reported results are the average value.

Preparation supported ionic liquid membranes (SILMs)

Durapore porous hydrophobic poly(vinylidene fluoride) (PVDF) membrane, with a pore size of 0.22 μm, average thickness of 125 μm, acquired from Millipore Corporation (USA) was only used to support the pure $[C_2mim][NTf_2]$. PVDF membrane filters have extensively been used in other works for the same purpose.[24,28,32] What is more, Neves *et al.* demonstrated that the stability of the hydrophobic PVDF membrane is larger than that of the hydrophilic.[27] Even though these membrane filters are characterized by their chemical resistance, we found that the impregnation of $[C_2mim][DCA]$, $[C_2mim][Ac]$, $[C_2mim][Lac]$ or $[C_2mim][SCN]$ into the pores of hydrophobic PVDF resulted in unstable SILMs. In order to overcome this drawback and improve the chemical resistance and compatibility of the support, porous hydrophilic poly(tetrafluoroethylene) (PTFE) membranes provided by Merck Millipore, with a pore size of 0.2 μm and average thickness of 65 μm, were used to prepare all the SILMs which are made of ILs containing the $[DCA]^-$, $[Ac]^-$, $[Lac]^-$ or $[SCN]^-$ anions.

To achieve stable SILMs, much care should be taken to ensure that the liquid sample completely fills the membranes pores. In this work, the SILM configuration process only used 1 mL of the pure ILs or their mixtures (previously dried). First, the membrane filter was introduced inside a vacuum chamber for 1 h in order to remove the air within the pores and facilitate the membrane wetting. Then, drops of the IL sample were spread on the membrane surface using a syringe, while keeping the vacuum inside the chamber. As the liquid penetrated into the membrane pores, the membrane became transparent. The SILM was left inside the chamber under vacuum for another 1 h. Finally, the SILM was taken out of the chamber and the excess of IL was wiped from the membrane surfaces with paper tissue. The amount of the sample immobilized was determined gravimetrically by weighing the membrane filter before and after impregnation. The membrane thickness was also confirmed using a digital micrometer (Mitutoyo, model MDE-25PJ, Japan). From gas permeation measurements it was obvious if the liquid did not completely fills the membrane pores.

Gas permeation measurements

Experimental measurements of CO_2, CH_4 and N_2 permeation through the prepared SILMs were conducted for single gas feed using a time-lag apparatus, construction and operation details on which are entirely described elsewhere.[68] Briefly, this system consists of two chambers (feed and permeate) separated by the permeation cell. Each prepared SILM was positioned on the top of a highly porous sintered disk for providing mechanical stability and installed into the permeation cell where it was degassed under vacuum during 12 h before testing. The gas permeation experiments were performed at 293 K with an upstream pressure of 100 kPa (feed) and vacuum (<0.1 kPa) as the initial downstream pressure (permeate). All permeation values are the result of at least three separate experiments of each gas on a single SILM sample. Between experiments, the permeation cell and lines were evacuated on both upstream and downstream sides until the pressure was below 0.1 kPa. The thickness of the SILM was assumed to be equivalent to the membrane filter thickness. No corrections were made for the tortuosity of the polymer membrane support.

Acknowledgements

Liliana C. Tomé is grateful to FCT (*Fundação para a Ciência e Tecnologia*) for her PhD research grant (SFRH/BD/72830/2010). Isabel M. Marrucho acknowledges FCT/MCTES (Portugal) for a contract under *Programa Ciência 2007*. This work was partially supported by FCT through the projects PTDC/EQU-FTT/116015/2009, Pest-OE/EQB/LA0004/2011 (ITQB) and Pest-C/CTM/LA0011/2011 (CICECO).

Notes and References

1 D. M. D'Alessandro, B. Smit and J. R. Long, *Angew. Chem., Int. Ed.*, 2010, **49**, 6058–6082.
2 A. D. Ebner and J. A. Ritter, *Sep. Sci. Technol.*, 2009, **44**, 1273–1421.
3 J. A. Velasco, L. Lopez, M. Velásquez, M. Boutonnet, S. Cabrera and S. Järås, *J. Nat. Gas Sci. Eng.*, 2010, **2**, 222–228.
4 H. Yang, Z. Xu, M. Fan, R. Gupta, R. B. Slimane, A. E. Bland and I. Wright, *J. Environ. Sci.*, 2008, **20**, 14–27.
5 A. Brunetti, F. Scura, G. Barbieri and E. Drioli, *J. Membr. Sci.*, 2010, **359**, 115–125.

6 L. M. Robeson, *J. Membr. Sci.*, 2008, **320**, 390–400.
7 F. F. Krull, C. Fritzmann and T. Melin, *J. Membr. Sci.*, 2008, **325**, 509–519.
8 M. J. Earle, J. M. S. S. Esperanca, M. A. Gilea, J. N. Canongia Lopes, L. P. N. Rebelo, J. W. Magee, K. R. Seddon and J. A. Widegren, *Nature*, 2006, **439**, 831–834.
9 J. L. Anderson, R. Ding, A. Ellern and D. W. Armstrong, *J. Am. Chem. Soc.*, 2004, **127**, 593–604.
10 M. Smiglak, W. M. Reichert, J. D. Holbrey, J. S. Wilkes, L. Sun, J. S. Thrasher, K. Kirichenko, S. Singh, A. R. Katritzky and R. D. Rogers, *Chem. Commun.*, 2006, 2554–2556.
11 M. A. Malik, M. A. Hashim and F. Nabi, *Chem. Eng. J.*, 2011, **171**, 242–254.
12 W. Zhao, G. He, F. Nie, L. Zhang, H. Feng and H. Liu, *J. Membr. Sci.*, 2012, **411–412**, 73–80.
13 C. Cadena, J. L. Anthony, J. K. Shah, T. I. Morrow, J. F. Brennecke and E. J. Maginn, *J. Am. Chem. Soc.*, 2004, **126**, 5300–5308.
14 J. E. Bara, T. K. Carlisle, C. J. Gabriel, D. Camper, A. Finotello, D. L. Gin and R. D. Noble, *Ind. Eng. Chem. Res.*, 2009, **48**, 2739–2751.
15 M. Hasib-ur-Rahman, M. Siaj and F. Larachi, *Chem. Eng. Process.*, 2010, **49**, 313–322.
16 M. Ramdin, T. W. de Loos and T. J. H. Vlugt, *Ind. Eng. Chem. Res.*, 2012, **51**, 8149–8177.
17 R. D. Rogers and K. R. Seddon, *Science*, 2003, **302**, 792–793.
18 N. V. Plechkova and K. R. Seddon, *Chem. Soc. Rev.*, 2008, **37**, 123–150.
19 P. Scovazzo, J. Kieft, D. A. Finan, C. Koval, D. DuBois and R. Noble, *J. Membr. Sci.*, 2004, **238**, 57–63.
20 R. E. Baltus, B. M. Counce, B. H. Culbertson, H. Lou, D. W. DePauli, S. Dai and C. Duckworth, *Sep. Sci. Technol.*, 2005, **40**, 525–541.
21 D. Morgan, L. Ferguson and P. Scovazzo, *Ind. Eng. Chem. Res.*, 2005, **44**, 4815–4823.
22 Y.-Y. Jiang, Z. Zhou, Z. Jiao, L. Li, Y.-T. Wu and Z.-B. Zhang, *J. Phys. Chem. B*, 2007, **111**, 5058–5061.
23 L. A. Neves, N. Nemestóthy, V. D. Alves, P. Cserjési, K. Bélafi-Bakó and I. M. Coelhoso, *Desalination*, 2009, **240**, 311–315.
24 P. Scovazzo, D. Havard, M. McShea, S. Mixon and D. Morgan, *J. Membr. Sci.*, 2009, **327**, 41–48.
25 P. Luis, L. A. Neves, C. A. M. Afonso, I. M. Coelhoso, J. G. Crespo, A. Garea and A. Irabien, *Desalination*, 2009, **245**, 485–493.
26 W. Zhao, G. He, L. Zhang, J. Ju, H. Dou, F. Nie, C. Li and H. Liu, *J. Membr. Sci.*, 2010, **350**, 279–285.
27 L. A. Neves, J. G. Crespo and I. M. Coelhoso, *J. Membr. Sci.*, 2010, **357**, 160–170.
28 P. Jindaratsamee, A. Ito, S. Komuro and Y. Shimoyama, *J. Membr. Sci.*, 2012, **423–424**, 27–32.
29 S. M. Mahurin, J. S. Yeary, S. N. Baker, D.-e. Jiang, S. Dai and G. A. Baker, *J. Membr. Sci.*, 2012, **401–402**, 61–67.
30 J. J. Close, K. Farmer, S. S. Moganty and R. E. Baltus, *J. Membr. Sci.*, 2012, **390–391**, 201–210.
31 L. Ferguson and P. Scovazzo, *Ind. Eng. Chem. Res.*, 2007, **46**, 1369–1374.
32 P. Cserjési, N. Nemestóthy and K. Bélafi-Bakó, *J. Membr. Sci.*, 2010, **349**, 6–11.
33 Y. Hou and R. E. Baltus, *Ind. Eng. Chem. Res.*, 2007, **46**, 8166–8175.
34 R. Condemarin and P. Scovazzo, *Chem. Eng. J.*, 2009, **147**, 51–57.
35 J. E. Bara, C. J. Gabriel, S. Lessmann, T. K. Carlisle, A. Finotello, D. L. Gin and R. D. Noble, *Ind. Eng. Chem. Res.*, 2007, **46**, 5380–5386.
36 J. E. Bara, C. J. Gabriel, T. K. Carlisle, D. E. Camper, A. Finotello, D. L. Gin and R. D. Noble, *Chem. Eng. J.*, 2009, **147**, 43–50.
37 T. K. Carlisle, J. E. Bara, C. J. Gabriel, R. D. Noble and D. L. Gin, *Ind. Eng. Chem. Res.*, 2008, **47**, 7005–7012.
38 P. Cserjési, N. Nemestóthy, A. Vass, Z. Csanádi and K. Bélafi-Bakó, *Desalination*, 2009, **245**, 743–747.
39 S. M. Mahurin, J. S. Lee, G. A. Baker, H. Luo and S. Dai, *J. Membr. Sci.*, 2010, **353**, 177–183.
40 S. M. Mahurin, P. C. Hillesheim, J. S. Yeary, D.-e. Jiang and S. Dai, *RSC Adv.*, 2012, **2**, 11813–11819.
41 H. Niedermeyer, J. P. Hallett, I. J. Villar-Garcia, P. A. Hunt and T. Welton, *Chem. Soc. Rev.*, 2012, **41**, 7780–7802.
42 S. Potdar, R. Anantharaj and T. Banerjee, *J. Chem. Eng. Data*, 2012, **57**, 1026–1035.
43 A. Finotello, J. E. Bara, S. Narayan, D. Camper and R. D. Noble, *J. Phys. Chem. B*, 2008, **112**, 2335–2339.
44 M. B. Shiflett and A. Yokozeki, *J. Chem. Eng. Data*, 2008, **54**, 108–114.
45 M. Wang, L. Zhang, L. Gao, K. Pi, J. Zhang and C. Zheng, *Energy Fuels*, 2012, **27**, 461–466.
46 C. Wu, T. P. Senftle and W. F. Schneider, *Phys. Chem. Chem. Phys.*, 2012, **14**, 13163–13170.
47 G. Wang, W. Hou, F. Xiao, J. Geng, Y. Wu and Z. Zhang, *J. Chem. Eng. Data*, 2011, **56**, 1125–1133.
48 B. F. Goodrich, J. C. de la Fuente, B. E. Gurkan, Z. K. Lopez, E. A. Price, Y. Huang and J. F. Brennecke, *J. Phys. Chem. B*, 2011, **115**, 9140–9150.
49 C. Wang, X. Luo, H. Luo, D.-e. Jiang, H. Li and S. Dai, *Angew. Chem., Int. Ed.*, 2011, **50**, 4918–4922.
50 M. J. Muldoon, S. N. V. K. Aki, J. L. Anderson, J. K. Dixon and J. F. Brennecke, *J. Phys. Chem. B*, 2007, **111**, 9001–9009.
51 X. Zhang, X. Zhang, H. Dong, Z. Zhao, S. Zhang and Y. Huang, *Energy Environ. Sci.*, 2012, **5**, 6668–6681.
52 J. G. Wijmans and R. W. Baker, *J. Membr. Sci.*, 1995, **107**, 1–21.
53 S. W. Rutherford and D. D. Do, *Adsorption*, 1997, **3**, 283–312.
54 J. Jacquemin, P. Husson, A. A. H. Padua and V. Majer, *Green Chem.*, 2006, **8**, 172–180.
55 K. R. Seddon, A. Stark and M. J. Torres, *Pure Appl. Chem.*, 2000, **72**, 2275–2287.
56 P. Scovazzo, *J. Membr. Sci.*, 2009, **343**, 199–211.
57 P. C. Hillesheim, S. M. Mahurin, P. F. Fulvio, J. S. Yeary, Y. Oyola, D.-e. Jiang and S. Dai, *Ind. Eng. Chem. Res.*, 2012, **51**, 11530–11537.
58 J. Albo, E. Santos, L. A. Neves, S. P. Simeonov, C. A. M. Afonso, J. G. Crespo and A. Irabien, *Sep. Purif. Technol.*, 2012, **97**, 26–33.
59 S. S. Moganty and R. E. Baltus, *Ind. Eng. Chem. Res.*, 2010, **49**, 9370–9376.
60 D. Camper, J. Bara, C. Koval and R. Noble, *Ind. Eng. Chem. Res.*, 2006, **45**, 6279–6283.

61 P. K. Kilaru and P. Scovazzo, *Ind. Eng. Chem. Res.*, 2007, **47**, 910–919.
62 G. Gurau, H. Rodríguez, S. P. Kelley, P. Janiczek, R. S. Kalb and R. D. Rogers, *Angew. Chem., Int. Ed.*, 2011, **50**, 12024–12026.
63 M. I. Cabaco, M. Besnard, Y. Danten and J. A. P. Coutinho, *J. Phys. Chem. A*, 2012, **116**, 1605–1620.
64 M. Besnard, M. I. Cabaco, F. V. Chavez, N. Pinaud, P. J. Sebastiao, J. A. P. Coutinho, J. Mascetti and Y. Danten, *J. Phys. Chem. A*, 2012, **116**, 4890–4901.
65 P. J. Carvalho and J. A. P. Coutinho, *Energy Environ. Sci.*, 2011, **4**, 4614–4619.
66 M. Tariq, P. J. Carvalho, J. A. P. Coutinho, I. M. Marrucho, J. N. C. Lopes and L. P. N. Rebelo, *Fluid Phase Equilib.*, 2011, **301**, 22–32.
67 X. Paredes, O. Fandiño, M. J. P. Comuñas, A. S. Pensado and J. Fernández, *J. Chem. Thermodyn.*, 2009, **41**, 1007–1015.
68 L. C. Tomé, D. Mecerreyes, C. S. R. Freire, L. P. N. Rebelo and I. M. Marrucho, *J. Membr. Sci.*, 2013, **428**, 260–266.